Turbulence in Flocculators: Effects of Tank Size and Impeller Type

Joel J. Ducoste and Mark M. Clark
Dept. of Civil Engineering, University of Illinois Urbana-Champaign, Urbana, IL 61801

Ronald J. Weetman
LIGHTNIN, Rochester, NY 14611

Past research shows that for the same power per unit volume, flocculation performance varies with tank size and impeller type. This study was performed to characterize effects of scale and impeller design on turbulence produced in the flocculation process. The study was performed with a Rushton turbine and an A310 foil impeller in three square tanks of 5-, 28- and 560-L volume. Fluid velocities were measured using a dual-channel laser Doppler velocimeter with an enhanced burst spectrum analyzer. Flocculation tanks were operated at a constant average unit-mass energy-dissipation rate of 0.0016 m^2/s^3. The results show that the turbulence intensity and local turbulent energy-dissipation rate were higher for the Rushton turbine than for the A310 impeller. The turbulence intensity was found to increase with increasing tank size regardless of impeller type. The local turbulent energy dissipation rate decreased for the Rushton turbine and remained constant for the A310 impeller with increasing tank size.

Introduction

The purpose of flocculation is to physically transform smaller particles into larger aggregates (flocs) that will eventually settle. Although Brownian motion, relative fluid motion from laminar shear or turbulence, and differential sedimentation can all lead to particle collisions in many unit processes in potable water treatment (Weber, 1972; Pontius, 1990), it is the fluid turbulence that controls the aggregation rate. As small particles become parts of larger aggregates, the flocs eventually reach sizes where the same relative fluid velocities that cause aggregation can also result in floc breakup.

Since the relative fluid velocities in the flocculation system control both aggregation and deaggregation rates, it is natural to imagine that changes in the levels of the velocity gradients will shift the equilibrium floc-size distribution just as temperature will shift a reversible chemical reaction one way or another. In the Kolmogoroff equilibrium theory, relative fluid velocities in the viscous dissipation and inertial subranges are both related to the turbulent unit mass-energy dissipation rate, ϵ. Therefore, when the average dissipation rate, $\bar{\epsilon}$, in various turbulent mixing systems is held constant, flocculation theory predicts the same equilibrium floc-size distribution.

There are several possible problems with this theory. First, it is difficult to establish exactly the spatial average ϵ for a turbulent mixing system. In most cases, we have estimated the average ϵ in terms of the total power, P, dissipated in mixing,

$$\bar{\epsilon} = \frac{P}{\rho \, \mathrm{Vol}}, \tag{1}$$

where ρ is the fluid density and Vol is the system volume. However, Tennekes and Lumley (1972) show that the total energy dissipated in a turbulent system is partitioned between the direct dissipation rate (due to mean velocity gradients) and the turbulent dissipation rate, ϵ. For high enough Reynolds numbers, the total dissipation rate is predicted to approach ϵ. There are, however, plenty of turbulent flows in which this may not be the case (Clark, 1985). Therefore, it is possible to imagine turbulent flocculation systems with the same P, but with different average ϵ.

Correspondence concerning this article should be addressed to M. M. Clark.
Present address of J. J. Ducoste: CH2M Hill, 625 Herndon Parkway, Herndon, VA 22070.

Second, two flocculation systems with the same spatial average $\bar{\epsilon}$ might have very different spatial distributions of energy dissipation rate and relative fluid velocities. It can be shown that the spatial average of the dissipation rates using Eq. 1 may not be the same as computing the global average of the local energy-dissipation rate when the heterogeneity of the turbulent field is considered (Clark, 1985). For example, if two different flocculation impellers consume the same amount of energy per unit time in the same size flocculation vessel but produce very different spatial distributions of ϵ and velocity gradients, then the equilibrium floc-size distributions would likely vary in the two systems. This problem in flocculation theory has not really been addressed adequately.

Another related problem is the variation in flocculation kinetics with scale. Consider now a single flocculation impeller design and two geometrically identical flocculation systems of different size but operated at the same average unit-mass energy-dissipation rate. Most flocculation kinetic schemes formulated in the past would predict no difference in the equilibrium floc-size distribution. As pointed out earlier, since most kinetic schemes do not consider spatial variations in dissipation rates and velocity gradients, then these theories will also not predict sensitivity to scale-related changes in the fluid mechanics. Some work in the emulsification area suggests that these scale-related changes may be significant. Konno et al. (1983) showed that the equilibrium drop-size distributions in different size vessels operated at the same unit-mass energy-dissipation rate are not equivalent, with larger breakup rates in larger vessels and a decrease in the average drop size with increasing system scale.

One crude statistical measure of the equilibrium floc-size distribution has been the maximum floc size, d_{max}. It has been shown by investigators (Thomas, 1964; Parker et al., 1972; Francois, 1987; Sonntag and Russel, 1987; Tambo and Francois, 1991; Kusters, 1991) that this steady-state maximum floc size is related to the average intensity of the turbulent fluid motion. While the complexity of this relationship varies with the investigator, all of the variations can be represented by the following equation:

$$d_{max} = \frac{C}{\bar{\epsilon}^n}, \tag{2}$$

where C is a coefficient related to the strength of the floc particles, and n is the coefficient related to the breakup mode, the size of eddies that cause the disruption in either the inertial or the viscous subrange regime of turbulence, and the fractal dimension of the floc aggregate. Setting $\bar{\epsilon}$ = constant, Eq. 2 would predict a maximum stable floc size regardless of tank size or impeller type. However, research done in flocculation scale-up by Oldshue and Mady (1978), Clark and Fiessinger (1991), and Clark et al. (1994) showed a degradation in flocculation performance with increasing tank size with $\bar{\epsilon}$ = constant. Other investigators have also found that for $\bar{\epsilon}$ = constant, the flocculation performance varies with impeller type (Drobny, 1963; Patwardham and Mirajgaonkar, 1970; Hanson and Cleasby, 1990; Clark et al., 1994; Sajjad and Cleasby, 1995).

There is growing evidence that a more complex relationship exists between particle agglomeration/breakup and the turbulence generated by a mixing impeller in a flocculation basin that cannot be fully described by Eq. 2. The inability of Eq. 2 to properly predict the flocculation performance may lie with the oversimplification of describing the three-dimensional nature of the turbulence with $\bar{\epsilon}$. To understand fully the relationship between agglomeration/breakup and turbulence, it is necessary to first characterize the turbulence in flocculators.

The objective of this study is to characterize the turbulence produced in the flocculation process by a mixing impeller. Mean and turbulent velocities and turbulent energy-dissipation rate were measured at several locations in square batch flocculators. The effect of changing the vessel size and impeller type on the fluid-mechanics properties measured at the different locations in the vessel were evaluated. The study was performed with Rushton turbines and A310 fluid-foil impellers in three square tanks of 5- ,28- and 560-L volume.

Experimental Methods

Measurement of the fluid velocities in the flocculation tank was done using a dual-channel laser Doppler velocimeter (LDV). LDV involves the measurement of fluid velocities by detecting the Doppler frequency shift of laser light that has been scattered by small particles moving with the fluid at one particular point. The LDV measurements were conducted at points shown in Figure 1. Because the flocculation tanks have square cross sections, an equivalent circle diameter (T) was calculated based on the cross-sectional area of the square tank. The computation of T was necessary to determine an impeller diameter over tank diameter ratio (D/T) for the flocculation tanks. The LDV measurements were conducted for the Rushton and A310 fluid-foil impellers at a (D/T) ratio of 0.33. The Rushton turbines and A310 foil impellers used in this study were built by LIGHTNIN. Table 1 displays some characteristic dimensions of both impellers. The Rushton turbine is a high-shear, high-power radial-flow impeller. The A310 foil impeller is a low-shear, hydrodynamically smooth axial-flow impeller designed and developed by LIGHTNIN. The A310 foil impeller design is based on airfoil technology (Abbot and Von Doenhoff, 1959). The operating conditions listed in Table 2 were tested at each point. The

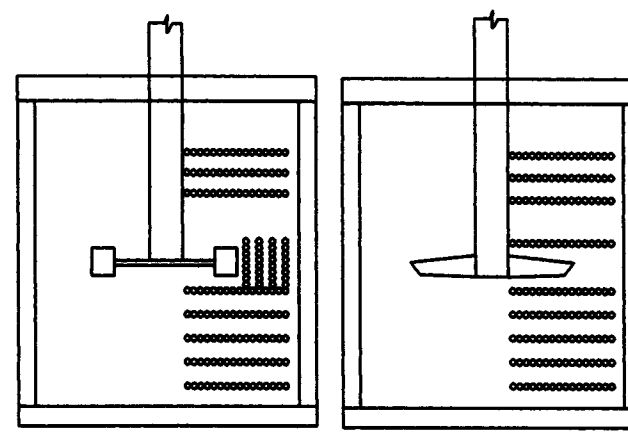

Figure 1. Location of LDV measurements for an axial (A310) and radial (Rushton) impeller.

Table 1. Characteristic Dimensions of the Rushton Turbine and A310 Foil Impeller

Rushton Turbine	A310 Foil Impeller
Blade width: 0.2 D	Tip chord angle: 22°
Blade thickness: 0.016 D	Width between leading and trailing edge
Blade length: 0.25 D	0.10 D at impeller tip
Disc diameter: 0.68 D	0.15 D at hub
Disc thickness: 0.016 D	Camber
Hub diameter: 0.24 D	0.05 D at impeller tip
Hub height: 0.14 D	0.0 D at impeller tip
	NACA Specification: 5,510

vessels were operated at $\bar{\epsilon} = 0.0016\ m^2/s^3$. This $\bar{\epsilon}$ is a typical average dissipation rate found in flocculation processes. At these operating conditions, the impeller Reynolds number is on the order of 10^4. This indicates that the flow regime during the flocculation process is turbulent. Measurement of the fluid velocities in the flocculation tanks were performed at LIGHTNIN in Rochester, New York. The Dantec type 60X two-color LDV, used at LIGHTNIN, allows measurement of two velocity components simultaneously.

The laser head is mounted on a computer-controlled traversing mechanism that allows the user to conduct a complete scan of the flocculation tank. The measurements are collected via backscattering, with both receiving and transmitting optics in the same module. Data acquisition and preprocessing of the particle velocity information are done using a DANTEC Burst Spectrum Analyzer (BSA). Computation of the mean velocity, rms fluctuating velocity, and turbulent energy-dissipation rate per unit mass are all done using a Fortran program implemented on a Hewlett-Packard 715/75 workstation.

The sizes of the LDV measuring volume diameter and length are 143 μm and 2.28 mm, respectively. A frequency shift of 40 MHz is used to determine the proper direction of the velocity vector at the measurement point. The fluid in the stirred tank was seeded with alumina particles with a mean particle size of 8 μm. The alumina particles were chosen because of alumina's high refractive index. With a maximum allowable error of 10%, an 8-μm alumina particle in water will follow fluctuations (Lagrangian) in the flow up to 16.5 kHz (Goldstein, 1983). An unbiased mean velocity and turbulent fluctuating velocity were computed by weighting each measurement with the burst time. Four thousand and ninety-six points were used to calculate the unbiased mean and turbulent fluctuating velocities.

The particle arrival times or the time a particle enters the measuring volume is random. The algorithm used to compute the autocorrelations and power spectra requires that the data input be equispaced in time. Therefore, a time trace of the 4,096 velocity measurements must be reconstructed. Typically, the velocity time trace is reconstructed using a simple sample-and-hold technique. The problem with this technique is

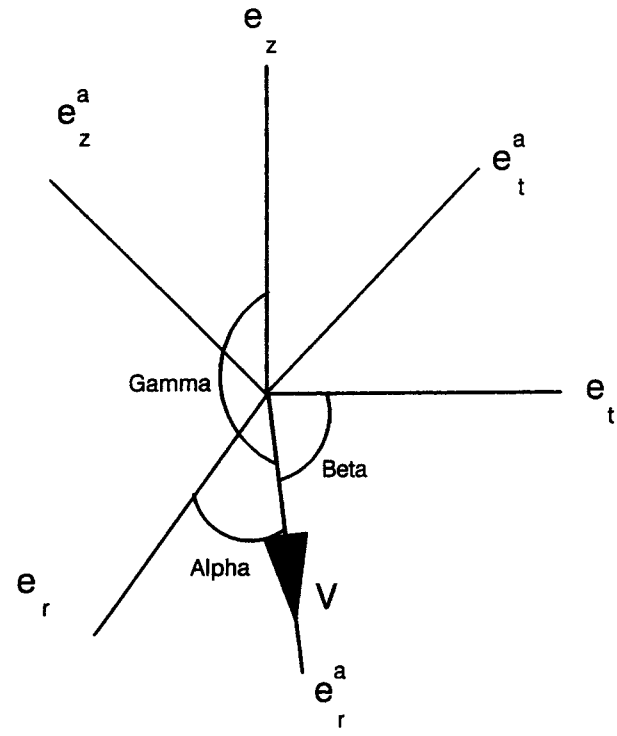

Figure 2. Coordinate transformation of the mean flow.

that the holding procedure masks the high-frequency information (Adrian and Yao, 1987). In order to increase the range of frequency from the fluctuating velocity data, Adrian and Yao (1987) recommend that better interpolation schemes such as linear or quadratic splines be used to reconstruct the velocity time trace. In this research, a linear interpolation scheme was used between particle arrival times. The power spectrum and the autocorrelation were computed by performing a fast Fourier transform (FFT) on the reconstructed data.

Computation of Resultant Fluctuating Velocity and Turbulent Energy-Dissipation Rate

Taylor (1938) first determined how to measure a characteristic size of the energy-containing eddies using the autocorrelation curve. An eddy is a large group of fluid particles that move laterally and longitudinally in the fluid flow. By using the autocorrelation curve, Taylor assumed that the eddy passed the point of measurement with the speed of the mean velocity (i.e., Taylor's frozen-field hypothesis). His experiments were conducted in a channel where the mean flow was primarily in one coordinate direction. In the flocculation tank, the mean flow will not be strictly in one coordinate direction. It will generally retain all three components of velocity.

Table 2. Operating Conditions for Each Impeller/Tank Configuration, $\bar{\epsilon} = 1.60 \times 10^{-3}\ m^2/s^3$

Impeller Type	$T = 5$ L $D = 2.5$ in. (64 mm) N (rev/min)	$T = 28$ L $D = 4.5$ in. (114 mm) N (rev/min)	$T = 557$ L $D = 12.8$ in. (325 mm) N (rev/min)
Rushton turbine	84.32	56.22	26.68
A310 fluid foil	173.9	115.94	55.02

In order to properly compute the integral length scale in the direction of the mean flow assuming Taylor's frozen-field hypothesis, a coordinate transformation can be done (Figure 2). As a result of a coordinate transformation, the mean flow will be in one direction in the new coordinate system. Once the mean flow is in one direction, the integral length scale (a characteristic size of the energy-containing eddy) can be easily computed along this direction.

Using Figure 2 as a guide, the new unit vectors e_r^a, e_t^a, e_z^a, are computed in terms of the original unit vectors e_r, e_t, e_z:

$$\begin{aligned} e_r^a &= Q_{rr}e_r + Q_{tr}e_t + Q_{zr}e_z \\ e_t^a &= Q_{rt}e_r + Q_{tt}e_t + Q_{zt}e_z \\ e_z^a &= Q_{rz}e_r + Q_{tz}e_t + Q_{zz}e_z \\ e_i^a &= Qe_i = Q_{mi}e_m. \end{aligned} \tag{3}$$

In essence, the two coordinate systems are related by an orthogonal tensor or transformation tensor, Q, shown as:

$$Q = \begin{bmatrix} Q_{rr} & Q_{tr} & Q_{zr} \\ Q_{rt} & Q_{tt} & Q_{zt} \\ Q_{rz} & Q_{tz} & Q_{zz} \end{bmatrix}.$$

To convert a velocity vector in the old coordinate system of the form

$$\bar{V} = V_r e_r + V_t e_t + V_z e_z$$

to the new coordinate system of the form

$$\overline{V^a} = V_r^a e_r^a + V_t^a e_t^a + V_z^a e_z^a,$$

we simply multiply the old velocity vector by the transformation tensor Q:

$$\begin{bmatrix} V_r^a \\ V_t^a \\ V_z^a \end{bmatrix}_{e^a} = \begin{bmatrix} Q_{rr} & Q_{tr} & Q_{zr} \\ Q_{rt} & Q_{tt} & Q_{zt} \\ Q_{rz} & Q_{tz} & Q_{zz} \end{bmatrix} \begin{bmatrix} V_r \\ V_t \\ V_z \end{bmatrix}_e.$$

Now, in the new coordinate system, we want the resultant velocity vector to exist only in one direction. As shown in Figure 2, the resultant velocity vector is arbitrarily chosen to be nonzero in the e_r^a direction only. Therefore, the resultant velocity vector in the new coordinate system is described as follows:

$$V_r^a = Q_{rr}V_r + Q_{tr}V_t + Q_{zr}V_z, \tag{4}$$

where

$$Q_{rr} = \frac{V_r}{\sqrt{V_r^2 + V_t^2 + V_z^2}} = \cos\alpha$$

$$Q_{tr} = \frac{V_t}{\sqrt{V_r^2 + V_t^2 + V_z^2}} = \cos\beta$$

$$Q_{zr} = \frac{V_z}{\sqrt{V_r^2 + V_t^2 + V_z^2}} = \cos\gamma,$$

where Q_{rr}, Q_{tr}, and Q_{zr} are also known as direction cosines. The next step is to compute the autocorrelation function of the turbulent velocity fluctuation in the radial direction in this new coordinate system. If we assume that:

$$V_r^a = \overline{V_r^a} + v_r^a,$$

where $\overline{V_r^a}$ represents the mean velocity component in new coordinate system and v_r^a represents the turbulent fluctuation velocity component in new coordinate system, then the correlation function, $\overline{v^a(t)\, v^a(t+\tau)}$, is defined by the following equation:

$$\begin{aligned} \overline{v_r^a(t)v_r^a(t+\tau)} &= \overline{v_r(t)\, v_r(t+\tau)}Q_{rr}^2 + \overline{v_t(t)v_t(t+\tau)}Q_{tr}^2 \\ &+ \overline{v_z(t)v_z(t+\tau)}Q_{zr}^2 + \left(\overline{v_r(t)v_t(t+\tau)} + \overline{v_t(t)v_r(t+\tau)}\right)Q_{rr}Q_{tr} \\ &+ \left(\overline{v_r(t)v_z(t+\tau)} + \overline{v_z(t)v_r(t+\tau)}\right)Q_{rr}Q_{zr} + \left(\overline{v_z(t)v_t(t+\tau)}\right. \\ &\left. + \overline{v_t(t)v_z(t+\tau)}\right)Q_{tr}Q_{zr}. \end{aligned} \tag{5}$$

The mean square of the velocity fluctuation in the radial direction in the new coordinate system is defined by the following equation:

$$\begin{aligned} (\sigma_r^a)^2 &= \sigma_r^2 Q_{rr}^2 + \sigma_t^2 Q_{tr}^2 + \sigma_z^2 Q_{zr}^2 + 2\overline{v_r v_t}Q_{rr}Q_{tr} \\ &+ 2\overline{v_r v_z}Q_{rr}Q_{zr} + 2\overline{v_z v_t}Q_{zr}Q_{tr}, \end{aligned} \tag{6}$$

where

σ_r^2 = mean square velocity fluctuation, old coordinate system, in radial direction
σ_t^2 = mean square velocity fluctuation, old coordinate system, in tangential direction
σ_z^2 = mean square velocity fluctuation, old coordinate system, in axial direction
$(\sigma_r^a)^2$ = mean square velocity fluctuation, new coordinate system, in radial direction

The autocorrelation coefficient of the velocity fluctuation in the radial direction in the new coordinate system is now defined by the following equation:

$$R_{v_r^a v_r^a}(\tau) = \frac{\overline{v_r^a(t)v_r^a(t+\tau)}}{(\sigma_r^a)^2}. \tag{7}$$

The integral length scale is then determined by integrating the preceding autocorrelation coefficient in the new coordi-

nate system with respect to τ, the time lag, and multiplying the result by the magnitude of the mean velocity. This is shown by the following equation:

$$L = |V_r^a| \int_0^\infty R_{v_r^a v_r^a}(\tau)\, d\tau. \tag{8}$$

Since the flocculation process operates at a high Reynolds number, the rate of energy dissipated at the small-scale eddies can be defined as the product of the energy flux across the large-scale eddies and the characteristic time of these large-scale eddies (Batchelor, 1953). From dimensional analysis, the energy flux across the large-scale eddies is on the order of $(\sigma_r^a)^2$, and the characteristic time of these eddies is on the order σ_r^a/L. Therefore, the energy dissipation rate, ϵ, is then computed by the following equation:

$$\epsilon = A\frac{(\sigma_r^a)^3}{L}, \tag{9}$$

where A is constant equal to 1 (Batchelor, 1953).

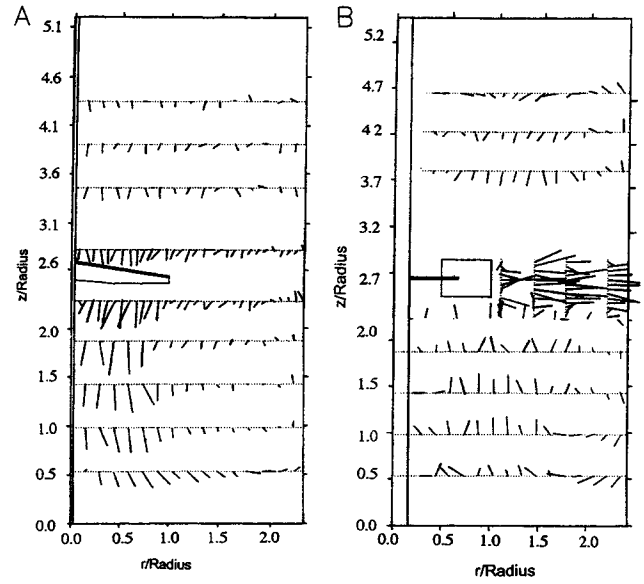

Figure 4. Mean velocity flow pattern.
(A) A310 foil impeller; (B) Rushton turbine.

Results

Mean velocity profile

The mean velocity profile at the impeller discharge boundary for the Rushton turbine and the A310 fluid-foil impeller are displayed in Figure 3. In Figure 3A, the mean velocity profile for the A310 foil impeller displays a sharp reduction in mean velocity near the center of the impeller ($r/R < 0.2$). The reduction in mean velocity near the center of the impeller is due to the proximity of the impeller hub at $r/R = 0 - 0.1$. The velocity profile for the foil impeller is almost constant between $r/R = 0.4$ and $r/R = 0.9$. In Figure 3B, the mean velocity profile for the Rushton turbine displays the familiar radial-jet profile (Kusters, 1991). Figure 3 also shows that when normalized by the impeller tip speed, the Rushton and A310 mean velocity profiles do not depend on the tank size.

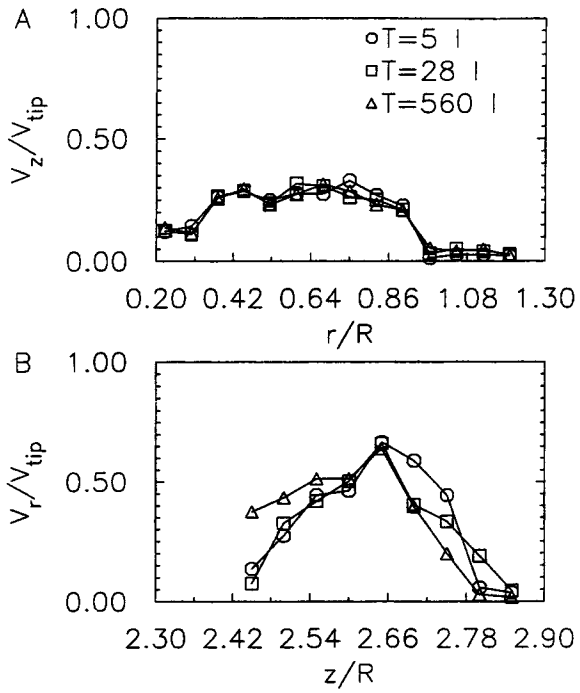

Figure 3. Mean velocity profile at the impeller discharge boundary.
(A) A310 foil impeller; (B) Rushton turbine.

The profiles of the resultant mean velocity vectors in the plane perpendicular to the tank wall are displayed in Figure 4 for the Rushton turbine and A310 foil impeller. In Figure 4A, the velocity profile, below the impeller centerline of the A310 foil impeller, is similar to that produced by other axial flow impellers. However, above the impeller centerline, the velocity profile near the tank wall seems to deviate from the flow pattern produced by a typical axial-flow impeller. Figure 4A seems to indicate that in the plane perpendicular to the tank wall, a circulation loop only exists below the impeller centerline. However, in order for the flow pattern to satisfy the continuity equation, fluid flow must circulate from the bottom to the top of the tank. Although no LDV measurements were taken close to the tank wall due to interference of the laser beams with the tank wall, it would seem that from visual observation of the free surface, most of the flow is circulating from the bottom to the top of the tank near the tank corners. However, more LDV measurements would be necessary to confirm this observation. The profile of the Rushton turbine shown in Figure 4B is typical of a radial-flow impeller (Desouza and Pike, 1972; Costes and Couderc, 1988; Weetman and Oldshue, 1988; Kusters, 1991). The flow patterns shown in Figure 4 were found to be the same at the three different tank sizes investigated in this study.

Resultant rms turbulent fluctuating velocity

The resultant rms turbulent fluctuating velocity in the direction of the mean flow was determined at each point using Eq. 6. In these experiments, the Reynolds shear stresses were

neglected in the computation of the resultant rms value. The LDV system was not set up to compute the Reynolds shear stresses (i.e., $\overline{u_i u_j}$ for $i \neq j$) used in Eq. 6. In order to properly compute the Reynolds shear stresses, each data point in the velocity time trace for each direction must be sampled at the same time. This was not possible with the LDV system used.

In general, the error in approximating the resultant rms value using Eq. 6 without the Reynolds shear stress is highest where the turbulent flow is anisotropic and lowest where the flow is isotropic. Studies done in shear layers where the turbulence is anisotropic have shown the following relationship (Hudson, 1993):

$$\overline{u_i u_j} \approx 0.45 \sigma_i \sigma_j,$$

where σ_i represents the rms fluctuating velocity in the i direction σ_j represents the rms fluctuating velocity in the j direction. In isotropic turbulence the constant 0.45 goes down to 0.1.

Ito et al. (1974, 1975) did some three-dimensional measurements of the velocity in a stirred tank with a Rushton turbine using a spherical electrode probe. Along with measuring the mean velocity and the rms fluctuating velocity, Ito et al. (1974, 1975) also measured the Reynolds shear stresses. They found that in the impeller discharge region, the magnitude of the Reynolds shear stress was about 25 to 50% of the mean square fluctuating velocity (i.e., $\overline{u_i u_j} \approx 0.5 \overline{u_i^2}$). This value occurred closest to the impeller tip. However, away from the impeller tip and in the bulk region, the magnitude of the Reynolds shear stress was about 0 to 5% of the mean square fluctuating velocity.

Another important problem with leaving out the Reynolds shear stresses from Eqs. 5–8 is in the usage of Eq. 9 to calculate the local energy dissipation rate. Recall that in order to use Eq. 9, the local turbulent Reynolds number must be sufficiently large. By leaving out the Reynolds shear stresses in the calculation of the turbulence intensity and length scales in the impeller discharge region, the local turbulent Reynolds number may not be large enough to compute the energy dissipation rate from dimensional analysis. So to assure that Eq. 9 could be used in the impeller discharge region, the local Reynolds number was computed for both the Rushton turbine and A310 foil impeller. The local Reynolds number was calculated using the local turbulence intensity and the characteristic integral length scale of the energy-containing eddies (Hinze, 1975). Table 3 displays the average local turbulent Reynolds number in the impeller discharge region of the Rushton turbine for the three different tank sizes. As Table 3 suggests, the local turbulent Reynolds number is on the order of 10^3, which is high enough to use Eq. 9 (Tennekes and Lumley, 1972; Hinze, 1975). The same order of magnitude was found for the local turbulent Reynolds number in the impeller discharge region of the foil impeller.

Clearly, the results from Ito et al. (1974, 1975) and Hudson (1993) suggest that leaving out the Reynolds shear stress can impact the accuracy of Eq. 6 only near the impeller blade tip. Also the high values of the local turbulent Reynolds number in Table 3 indicate that leaving out the Reynolds shear stress does not affect the use of Eq. 9 for calculating the local turbulent-energy dissipation rate. In the bulk region, the contribution of the Reynolds shear stress is negligible. The beauty

Table 3. Average Local Turbulent Reynolds for the Rushton Turbine in the Impeller Discharge Region

r/R	T = 5 L	T = 28 L	T = 560 L
1.1	4,610	5,915	8,079
1.444	4,469	8,366	11,817
1.778	3,546	4,805	7,271
2.222	2,557	4,628	8,344

of Eq. 6 is that for the first time, it provides a simple way to compute the resultant rms fluctuating velocity in the direction of the mean flow in stirred tanks. This method is also more consistent with Taylor's frozen-field hypothesis than the previous methods used for calculating the turbulence in stirred tanks. However, the accuracy of using Eq. 6 to compute the rms fluctuating velocity in the direction of the mean flow in the impeller discharge zone would be improved by the addition of these Reynolds shear stresses.

In the course of measuring the rms fluctuating velocity near the impeller tip, a periodic velocity component was found due to the pumping action of the impeller. This periodic velocity has the ability to inflate the value of the rms fluctuating velocity and cause "pseudoturbulence." Clearly, the periodic velocity is not a turbulent quantity and must be removed in order to compute the true rms fluctuating velocity. In this study, a digital Butterworth band-pass filter (Beauchamp and Yuen, 1979) was used to remove the specific frequencies of the periodic velocities. These frequencies were found to coincide with the blade passage frequency and its harmonics.

Figure 5A and 5B display the results of the resultant rms turbulent fluctuating velocity for the Rushton turbine in three square tanks. These results seem to indicate that when the rms fluctuating velocity is normalized by the impeller tip speed, the rms fluctuating velocity does not depend on the tank size. However, it is clear that the rms fluctuating velocity is a function of the location of measurement in the square tank. Figure 5A shows that the rms fluctuating velocity is about 8 to 10% of the impeller tip speed in the bulk region below the impeller. Figure 5B, however, shows that the rms fluctuating velocity is about 10 to 20% of the impeller tip speed in the impeller discharge region.

Figure 5C displays the resultant rms turbulent fluctuating velocities for the A310 foil impeller in three square tanks. These results also indicate that when the rms fluctuating velocity is normalized by the impeller tip speed, the rms value does not depend on the tank size. It only depends on the location of the measurement in the square tank. In Figure 5C, the rms fluctuating velocity is about 6 to 8% of the impeller tip speed below the foil-impeller discharge region. The results for the rms fluctuating velocity indicate that there is a difference between the Rushton turbine and the A310 foil impeller. Clearly, Figures 5A, 5B, and 5C suggest that for the same power per unit volume, the intensity of turbulence for the Rushton turbine is higher than for the A310, particularly in the impeller discharge zone. While the turbulence intensity is also higher in the bulk region of the tank for the Rushton than for the A310, the difference is not as great.

Turbulent energy-dissipation rate

The turbulent energy-dissipation rate per unit mass was computed using Eq. 9. Figures 6A and 6B display the results

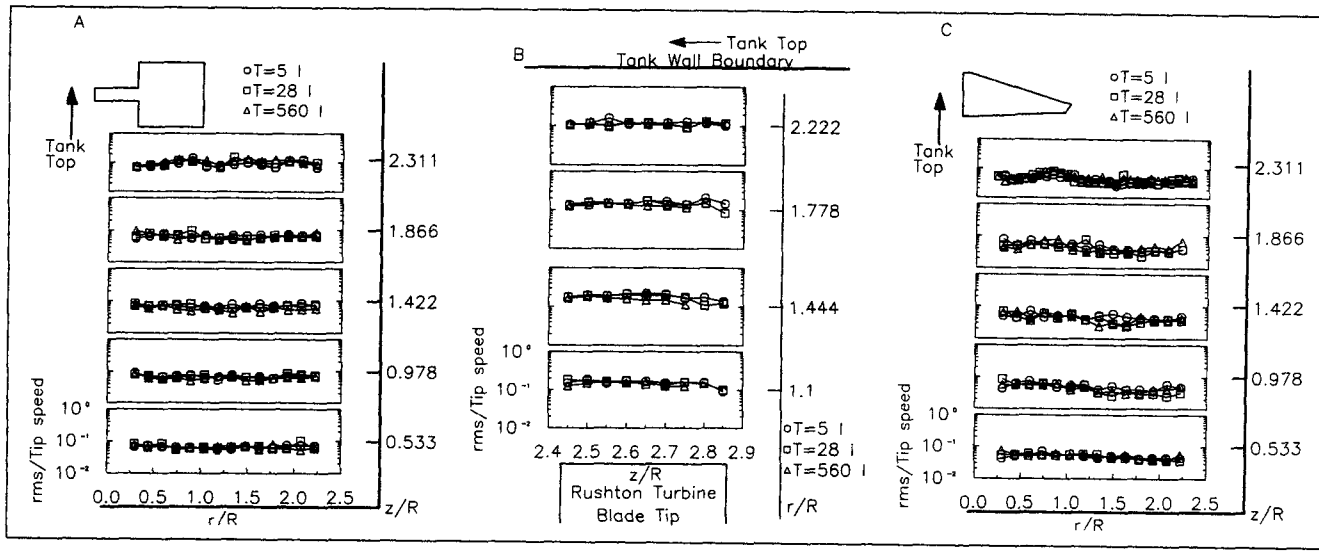

Figure 5. Resultant RMS turbulent fluctuating velocity in the direction of the mean flow.

(A) Rushton turbine below the impeller centerline; (B) Rushton turbine in the impeller discharge region; (C) A310 foil impeller below the impeller centerline.

of the energy-dissipation rate for the Rushton turbine at $T = 5$ L, $T = 28$ L, and $T = 560$ L. In these figure parts, the local energy-dissipation rate is normalized by the average energy-dissipation rate in the tank. Figures 6A and 6B show that at the locations measured, the local energy-dissipation rate decreases with increasing tank size. The average local energy-dissipation rate in the bulk region of the tank is about 81%, 54%, and 35% of the tank average energy-dissipation rate for $T = 5$ L, $T = 28$ L, and $T = 560$ L, respectively. In the impeller region, the average local energy-dissipation rate is about 12.5 times, 7.6 times, and 3.5 times the tank average energy-dissipation rate.

Figure 6C displays the local energy-dissipation rate for the A310 foil impeller at $T = 5$ L, $T = 28$ L, and $T = 560$ L. The results for the local energy-dissipation rate for the foil impeller do not show a clear difference between the tank sizes like the Rushton turbine results. In the impeller region, the local energy-dissipation rate is about 1.55 times, 1.43 times, and 1.66 times the tank average energy-dissipation rate for $T = 5$ L, $T = 28$ L, and $T = 560$ L, respectively. In the bulk region, these values are 75, 66 and 68%.

These results seem to indicate that for the A310 foil impeller, the local energy dissipation is not very sensitive to tank size. However, for the Rushton turbine, the local energy-

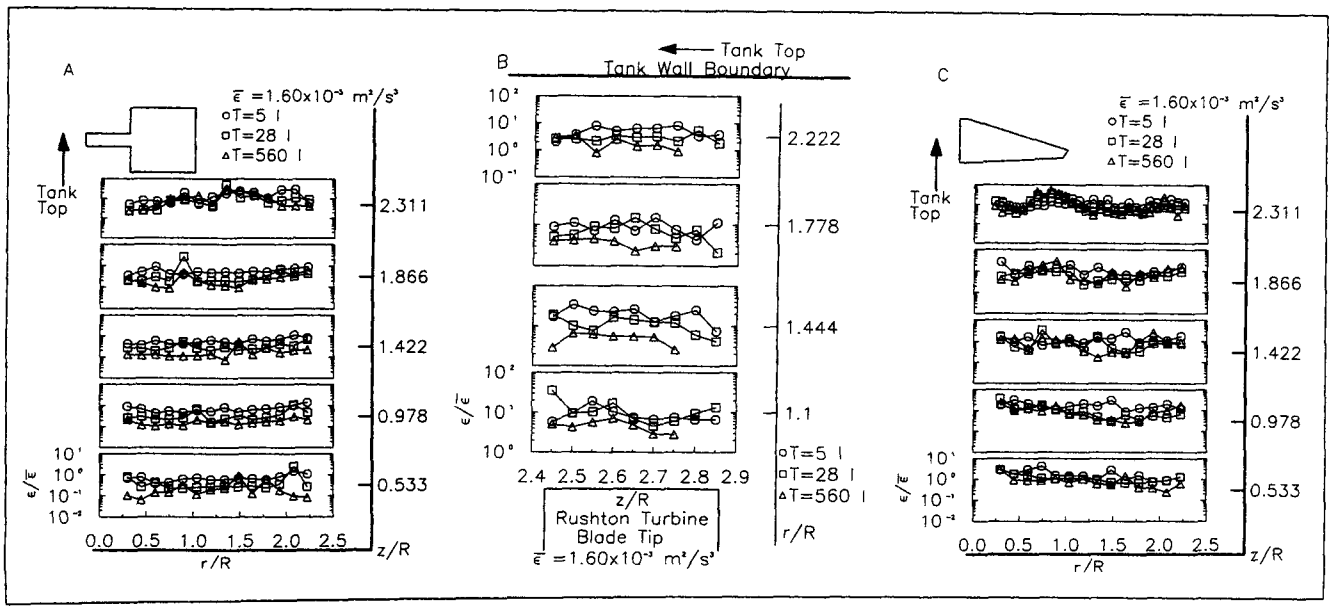

Figure 6. Turbulent energy dissipation rate.

(A) Rushton turbine below the impeller centerline; (B) Rushton turbine in the impeller discharge zone; (C) A310 foil impeller below the impeller centerline.

dissipation rate is sensitive to tank size, as seen by the results in Figures 6A and 6B. Clearly, these results show that for the same power per unit volume, the local energy-dissipation rate produced by the Rushton turbine is much higher in the impeller discharge region than the local energy-dissipation rate produced in the impeller discharge zone of the A310 foil impeller.

Discussion

The results from the LDV experiments indicate that maintaining constant average power per unit volume ($\bar{\epsilon}$ = constant) between different tank sizes or different impeller types does not translate to constant spatial distribution of the local turbulent flow properties. When $\bar{\epsilon}$ was kept constant, the rms fluctuating velocity was found not to depend on tank size when it was normalized by impeller tip speed. However, by maintaining $\bar{\epsilon}$ = constant, dimensional analysis predicts that the impeller tip speed increases with tank size as:

$$\frac{TS_l}{TS_s} \propto \left(\frac{T_l}{T_s}\right)^{1/3}, \tag{10}$$

where
TS = tip speed
T = tank side dimension
subscript l = large tank
subscript s = small tank

In the results section, the LDV experimental results (Figure 5) showed that the rms fluctuating velocity was proportional to the tip speed:

$$\frac{\text{rms}_l}{\text{rms}_s} \propto \left(\frac{TS_l}{TS_s}\right). \tag{11}$$

Substituting Eq. 10 in Eq. 11, the rms value is related to the tank dimension as

$$\frac{\text{rms}_l}{\text{rms}_s} \propto \left(\frac{T_l}{T_s}\right)^{1/3}. \tag{12}$$

Therefore, maintaining $\bar{\epsilon}$ = constant caused the rms fluctuating velocity to increase with tank size. Also, the spatial distribution of the dimensionless rms fluctuating velocity was much different between the Rushton turbine and the A310 foil impeller, particularly in the impeller discharge zone. For $\bar{\epsilon}$ = constant, the dimensionless rms fluctuating velocities or turbulence intensities were lower for the A310 foil impeller than for the Rushton turbine (Figure 5). The differences in the rms fluctuating velocity between the Rushton turbine and the A310 impeller are consistent with the turbulence results for the A310 impeller and the Rushton turbine reported by Weetman and Oldshue (1988). Part of Weetman and Oldshue's (1988) report showed a velocity time trace at the impeller outlet for the Rushton turbine and the A310 foil impeller. Their velocity time-trace results showed that the Rushton turbine produces a higher peak-to-peak fluctuating velocity component than the A310 foil impeller. This indicates that the turbulence generated by the Rushton turbine is greater than the turbulence produced by the A310 impeller.

Although the turbulent fluctuating velocities were found to increase with increasing tank size, the local turbulent energy-dissipation rate behaved quite differently. At the beginning of this research, the authors expected the local energy-dissipation rate to remain constant with increasing tank size since the power per unit volume was kept constant with increasing tank size (i.e., $\bar{\epsilon}$ = constant). Given constant power per unit volume for all three vessels, the spectral energy transfer from the large-scale eddies to the small-scale eddies should remain constant. Therefore, the energy dissipated at the small-scale eddies to heat should be the same regardless of the tank size when $\bar{\epsilon}$ = constant.

For the Rushton turbine, however, the local energy-dissipation rate was found to decrease with increasing tank size as

$$\frac{\epsilon_{\text{loc},l}}{\epsilon_{\text{loc},s}} \propto \left(\frac{T_l}{T_s}\right)^x, \tag{13}$$

where

$x = -0.70$ between 5-L and 28-L-tank bulk region
$x = -0.44$ between 28-L and 560-L-tank bulk region
$x = -0.85$ between 5-L and 28-L-tank impeller region
$x = -0.78$ between 28-L and 560-L-tank impeller region

This decreasing trend of the local energy-dissipation rate with increasing tank size does not seem consistent with maintaining constant power per unit volume with tank size. On the contrary, for the A310 foil impeller, the local energy-dissipation rate did not show any clear sensitivity to tank size. This constant energy-dissipation rate with increasing tank size is expected since the impeller power per unit volume has been kept constant. One possible reason for a decreasing local energy-dissipation rate with increasing tank size for the Rushton turbine might be due to the influence of the trailing vortices on the small-scale eddies.

Van't Riet and Smith (1975) have shown that a significant portion of the turbulent kinetic energy produced by the Rushton turbine is in the form of trailing vortices. This author speculates that as the tank size increases with $\bar{\epsilon}$ = constant, the contribution of the energy transformed from the trailing vortices to the small-scale eddies decreases with increasing tank size. This reduction in energy transfer from the trailing vortices to the small-scale eddies with tank size might be due to either a change in the location of the vortex axis or due to a decrease in the rate of vortex production.

Yianneskis et al. (1987) showed that for the same Reynolds number region studied by Van't Riet and Smith (1975) (i.e., $5\times10^3 < Re < 9\times10^4$), the location of the trailing vortex axis was found to be closer to the Rushton turbine blade tip for a larger impeller diameter. Results of Yianneskis et al. (1987) suggest that if the vortex axis is closer to the impeller, there would be less interaction between the trailing vortices and the flow regime in the impeller discharge region and the bulk region with increasing tank size. Consequently, the energy transferred from these vortices down to the small-scale eddies would decrease in these regions.

It is also possible that the increase or decrease in the interaction between the trailing vortices and the flow regime might be due to the number of vortices produced per unit time. If we assume that a trailing vortex is produced each time a blade passes a specific point, then we can conclude that the frequency of vortex production is equal to the blade passage frequency. Since the blade passage frequency decreases with increasing tank size when $\bar{\epsilon}$ = constant, we can expect the frequency of vortex production to also decrease with increasing tank size. Therefore, the energy transferred from these vortices down to the small-scale eddies would also decrease with tank size. Since there are no significant trailing vortices found for the A310 foil impeller due to its hydrodynamic shape and smooth leading edge, the energy dissipated at the small-scale eddy size was not a function of tank size.

The LDV experimental results seem to suggest that if there is an increase in floc breakup with increasing tank size, then the explanation may lie with how the turbulent fluctuating velocity influences floc breakup, and not with the turbulent energy-dissipation rate. The LDV experimental results have shown a clear increase in turbulent fluctuating velocity with tank size. However, the LDV results also showed either a decrease in the local energy-dissipation rate with increasing tank size for the Rushton turbine or no change in local energy-dissipation rate with tank size for the foil impeller when $\bar{\epsilon}$ = constant. This decrease or constant trend in the local energy-dissipation rate cannot explain the poorer flocculation performance found by other investigators (Oldshue and Mady, 1978; Clark and Fiessinger, 1991; Clark et al., 1994).

Implication of Experimental Results on Flocculation Performance

Several experiments have been done by previous investigators that showed that an inverse relationship exists between the maximum stable floc-size developed during the flocculation process and $\bar{\epsilon}$. However, experiments done by Oldshue and Mady (1978), Clark and Fiessinger (1991), and Clark et al. (1994) have shown that maintaining $\bar{\epsilon}$ = constant with increasing tank size or different impeller types does not produce similar flocculation performance. In fact, all three reports indicate a tendency for the flocculation performance to decrease with increasing tank size.

This decrease in flocculation performance is probably due to an increase in the breakup of floc particles with increasing tank size rather than a decrease in the agglomeration of floc particles. Researchers know that the breakup of floc particles ultimately determines the performance of the flocculation process since there is experimental evidence of a maximum stable floc size. The maximum stable floc size occurs when the agglomeration rate is balanced by the breakup rate of the floc particle. Researchers continue to use Eq. 2 to predict the maximum stable floc size, given $\bar{\epsilon}$. However, Eq. 2 cannot explain the shift to a lower maximum stable floc size due to increasing the vessel size when $\bar{\epsilon}$ = constant. A lower maximum stable floc size indicates an increase in the flocculation breakup rate. Therefore, something must have changed in the fluid mechanics to cause a change in the breakup rate of the floc particles even with $\bar{\epsilon}$ = constant.

The results of the LDV experiments suggests that by maintaining $\bar{\epsilon}$ = constant, the rms turbulent fluctuating velocity increased with increasing tank size regardless of impeller type. Those same experiments also indicate that for the Rushton turbine, the local energy-dissipation rate decreases with increasing tank size, and for the A310 foil impeller, the dissipation rate remains the same. These results seem to indicate that if floc breakage is increasing with tank size, it could be due to the difference between the turbulent fluctuating velocities across the aggregate diameter and not the local energy-dissipation rate.

Some researchers may argue that the difference between the turbulent fluctuating velocities across the aggregate diameter and the local energy-dissipation rate are related to each other if local isotropic conditions exist (Delichatsios and Probstein, 1975; Tambo and Watanabe, 1979; Glasgow and Hsu, 1979; Kusters, 1991). Batchelor (1953), Tennekes and Lumley (1972), and Hinze (1973) mentioned that when the Reynolds number is large, the small-scale structure of turbulence tends to be independent of any orientation effects introduced by the large-scale motion. Therefore, local isotropy at the small scale can be assumed. At these small scales of motion, the length scales and velocity scales can be uniquely defined by the energy-dissipation rate in the inertial subrange and by both the kinematic viscosity and the energy-dissipation rate below the Kolmogoroff microscale.

In developing the relationship between maximum floc size and $\bar{\epsilon}$, researchers assumed that the dynamics of agglomeration and breakup of particles occur at scales of motion in the universal equilibrium range. If agglomeration and breakup of particles occurred at these scales, then the resulting particle-size distribution should not be a function of the flocculator geometry. The effects of flocculator geometry such as tank size, impeller type, and tank shape only influence the large scales of motion. However, if breakup occurred at scales where the flow regime is anisotropic or at scales outside the universal equilibrium range, then the maximum floc size cannot be uniquely described by $\bar{\epsilon}$ and can be influenced by flocculator geometry.

Based on data from emulsification experiments, Konno et al. (1983) and Chang et al. (1981) displayed photographic evidence that a large portion of the oil droplets was broken behind the Rushton turbine blade. The breaking drops appeared to follow the outward flow along the impeller blade. This regularity in the direction of drop elongation would indicate that breakup occurred in the anisotropic turbulent region. Experimental and modeling results presented by Konno et al. (1983) and Chang et al. (1981) suggest that the rms turbulent fluctuating velocities in regions where the flow regime is anisotropic could be important in the breakup of floc particles. Therefore, an increase in the rms fluctuating velocity with increasing tank size, as shown in this study, could explain why investigators have seen a degradation in flocculation performance with increasing tank size.

If the rms turbulent fluctuating velocity in the impeller discharge zone is important in the breakup of floc particles, then the correct scale-up law may depend more on impeller tip speed than $\bar{\epsilon}$, since the results from this study clearly show that the rms turbulent fluctuating velocity is proportional to the impeller tip speed. Some investigators (Oldshue and Trussell, 1991) may argue that for geometrically similar tanks and impellers, it is not possible to keep all tank properties (i.e., power, power per unit volume, impeller rpm, diameter,

tip speed, Reynolds number, Froude number, Weber number) constant upon scale-up with one of these parameters held constant. However, not all tank properties are important to the agglomeration and breakup of floc particles. It is possible that only certain properties may influence the breakup rate more adversely than others.

There is no question that the turbulent fluctuating velocities are important to the agglomeration and breakup of floc particles during the flocculation process. The issue seems to be whether the turbulent fluctuating velocity in the flow regime where the power is dissipated into heat is critical to both the agglomeration and breakup of floc particles. If the fluctuating velocities at the smallest scale of turbulence were the controlling factor, then engineers should be able to maintain the same rate agglomeration and breakup of floc particles by keeping the power per unit volume constant to the flocculator.

Clearly, past research results for flocculation in different tank sizes and with different impeller types does not support this theory. It is possible, however, that the turbulent fluctuating velocities at larger scales of turbulence may be important to the breakup of these floc particles. Although the magnitude of these fluctuating velocities at these larger scales of turbulence are harder to predict theoretically, the results from this study suggest that by adjusting the impeller tip speed, engineers could adjust the level of the large-scale turbulence. Hence from this study, it is likely that the breakup rate in the flocculation process can be manipulated by simply adjusting the impeller tip speed.

Conclusions

Results of the fluid mechanics generated in a square tank with a Rushton turbine or an A310 foil impeller for $\bar{\epsilon}$ = constant have demonstrated the following:

- The mean velocities and rms turbulent fluctuating velocities are proportional to the impeller tip speed.
- The dimensionless rms turbulent fluctuating velocity is lower for the A310 fluid-foil impeller than for the Rushton turbine.
- The rms turbulent fluctuating velocity has been shown to increase with tank size as $D^{1/3}$. This was true regardless of impeller type.
- The local energy-dissipation rate for the Rushton turbine was found to decrease with increasing tank size as D^{-x}, where

$x = 0.70$ in bulk region between $T = 5$ L and $T = 28$ L
$x = 0.44$ in bulk region between $T = 28$ L and $T = 560$ L
$x = 0.85$ in impeller region between $T = 5$ L and $T = 28$ L
$x = 0.78$ in impeller region between $T = 28$ L and $T = 560$ L

- The local energy-dissipation rate for the A310 fluid-foil impeller did not vary with tank size.
- The local energy-dissipation rate in the impeller discharge zone of the A310 foil impeller was found to be much lower than the local energy-dissipation rate produced in the impeller discharge zone of the Rushton turbine.

Acknowledgments

This work was supported by the National Science Foundation (BCS-90-57387 PYI) and LIGHTNIN, a unit of General Signal. The authors would like to extend their sincere gratitude to Dr. Ronald J. Adrian for his insight on performing turbulence measurements in mixing vessels and his recommendation for the coordinate transformation.

Notation

$\overline{v_r v_t}$ = radial–tangential Reynolds shear stress, m^2/s^2
$\overline{v_r v_z}$ = radial–axial Reynolds shear stress, m^2/s^2
$\overline{v_z v_t}$ = axial–tangential Reynolds shear stress, m^2/s^2
$\bar{V}$ = resultant mean velocity, m/s
V = instantaneous velocity, m/s
α, β, γ = direction cosine angles
δ_{ij} = Kronecker delta
μ = dynamic viscosity, kg/m·s

Literature Cited

Abbot, I. H., and A. E. Von Doenhoff, *Theory of Wing Sections*, Dover, New York, (1959).
Adrian, R. J., and C. S. Yao, "Power Spectra of Fluid Velocities Measured by Laser Doppler Velocimetry," *Exp. Fluids*, **5**, 17 (1987).
Batchelor, G. K., *The Theory of Homogeneous Turbulence*, Cambridge Univ. Press, Cambridge, England (1953).
Beauchamp, K., and C. Yuen, *Digital Methods for Signal Analysis*, Allen & Unwin, London (1979).
Chang, T. P. K., Y. H. E. Sheu, G. B. Tatterson, and D. S. Dickey, "Liquid Dispersion Mechanisms in Agitated Tanks: II. Straight Blade and Disc Style Turbines," *Chem. Eng. Commun.*, **10**, 215 (1981).
Clark, M. M., and F. Fiessinger, "Mixing and Scaleup," *Mixing in Coagulation and Flocculation*, AWWARF Rep., Denver, CO, p. 282 (1991).
Clark, M. M., R. M. Srivastava, J. S. Lang, R. R. Trussell, L. J. Mccollum, D. Bailey, J. D. Christie, and G. Stolarik, *Selection and Design of Mixing Processes for Coagulation*, AWWARF Rep., Denver, CO (1994).
Clark, M. M., "Critique of Camp and Stein, RMS Velocity Gradient," *J. Environ. Eng. ASCE*, **111**(6), 741 (1985).
Costes, J., and J. P. Couderc, "Study by Laser Doppler Anemometry of the Turbulent Flow Induced by a Rushton Turbine in a Stirred Tank: Influence of the Size of the Units I: Mean Flow and Turbulence," *Chem. Eng. Sci.*, **43**, 2765 (1988).
Delichatsios, M. A., and R. F. Probstein, "Coagulation in Turbulent Flow: Theory and Experiment," *J. Colloid Interf. Sci.*, **51**(3), 394 (1975).
Desouza, A., and R. W. Pike, "Fluid Dynamics and Flow Patterns in Stirred Tanks with a Turbine Impeller," *Can J. Chem. Eng.*, **50**, 15 (1972).
Drobny, N. L., "Effect of Paddle Design on Flocculation," *J. Sanit. Div. ASCE*, **89** (SA2), 17 (1963).
Francois, R. J., "Strength of Aluminum Hydroxide Flocs," *Water Resour.*, **21**(9), 1023 (1987).
Goldstein, R. J., *Fluid Mechanics Measurement*, Hemisphere, New York (1983).
Glasgow, L. A., and J. P. Hsu, "An Experimental Study of Floc Strength," *AIChE J.*, **28** (5), 779 (1979).
Hanson, A. T., and J. L. Cleasby, "The Effect of Temperature on Turbulent Flocculation: Fluid Dynamics and Chemistry," *J. Amer. Water Works Assoc.*, **82**(11), 56 (1990).
Hinze, J. O., *Turbulence*, McGraw-Hill, New York (1975).
Hudson, J. D., "The Effect of a Wavy Boundary on Turbulent Flow," PhD Thesis, Univ. of Illinois Urbana-Champaign (1993).
Ito, S., S. Urushiyama, and K. Ogawa, "Measurement of Three-Dimensional Fluctuating Liquid Velocities," *J. Chem. Eng. Japan*, **7**(6), 462 (1974).
Ito, S., K. Ogawa, and N. Yoshida, "Turbulence in Impeller Stream in a Stirred Vessel," *J. Chem. Eng. Japan*, **8**(3), 206 (1975).
Konno, M., M. Aoki, and S. Saito, "Scale Effects on Breakup Processes in Liquid-Liquid Agitated Tanks," *J. Chem. Eng. Jpn.*, **16**(4), 312 (1983).
Kusters, K. A., "The Influence of Turbulence on Aggregation of Small Particles in Agitated Vessels," PhD Diss., Univ. of Eindhoven, Eindhoven, The Netherlands (1991).

Oldshue, J. Y., and O. B. Mady, "Flocculation Performance of Mixing Impellers," *Chem. Eng. Prog.*, **74,** 103 (1978).
Oldshue, J. Y., and R. R. Trussell, "Design of Impellers for Mixing," *Mixing in Coagulation and Flocculation*, A. Amirtharajah and M. Clark, eds., American Water Works Research Foundation, Denver, CO (1991).
Parker, D. S., W. J. Kaufman, and D. Jenkins, "Floc Breakup in Turbulent Flocculation Processes," *J. Sanit. Div. ASCE*, **SA1**, 79 (1972).
Patwardham, S. V., and A. G. Mirajgaonkar, "Hydraulics of Flocculation and Paddle Characteristics," *J. Inst. Eng. India*, **50,** 60 (1970).
Pontius, F. W., *Water Quality and Treatment*, McGraw-Hill, New York (1990).
Sajjad, M. W., and J. L. Cleasby, "Effects of Impeller Geometry and Various Mixing Patterns on Flocculation Kinetics of Kaolin Clay using Ferric Salt," *Proc. Amer. Water Works Assoc. Conf.*, Anaheim, CA (1995).
Sonntag, R. C., and W. B. Russel, "Structure and Breakup of Flocs Subjected to Fluid Stresses: II. Theory," *J. Colloid Interf. Sci.*, **115,** 378 (1987).
Tambo, N., and R. J. Francois, "Mixing, Breakup, and Floc Characteristics," *Mixing in Coagulation and Flocculation*, A. Amirtharajah and M. Clark, eds., American Water Works Research Foundation, Denver, CO (1991).
Tambo, N., and Y. Watanabe, "Physical Aspect of Flocculation Process I: Fundamental Treatise," *Water Res.*, **13,** 409 (1979).
Taylor, G. I., "The Spectrum of Turbulence," *Proc. Roy. Soc.*, **A164,** 476 (1938).
Tennekes, H., and J. L. Lumley, *A First Course in Turbulence*, MIT Univ. Press, Cambridge, MA (1972).
Thomas, D. G., "Turbulent Disruption of Flocs in Small Particle Size Suspension," *AIChE J.*, **10**(4), 517 (1964).
Van't Riet, K., and J. M. Smith, "The Trailing Vortex System Produced by Rushton Turbine Agitators," *Chem. Eng. Sci.*, **30,** 1093 (1975).
Weber, W. J., *Physicochemical Processes for Water Quality Control*, Wiley, New York (1972).
Weetman, R. J., and J. Y. Oldshue, "Power, Flow, and Shear Characteristics of Mixing Impellers," *Eur. Conf. on Mixing*, Pavia, Italy (1988).
Yianneskis, M., Z. Popiolek, and J. H. Whitelaw, "An Experimental Study of the Steady and Unsteady Flow Characteristics of Stirred Reactors," *J. Fluid Mech.*, **175,** 537 (1987).

Manuscript received Oct. 31, 1995, and revision received July 15, 1996.